Chapter 7

General discussion and outlook

7.1 Structural assessment

Advances in the understanding of BChl biosynthesis in *C. tepdium* has led to the generation of a set of its mutants which can produce chlorosomes containing self-assembled BChl molecules of a single homologue. Cryo-EM studies on the WT and the *bchQRU* mutant of *C. tepidum* have revealed an increased suprastructural order in the mutant chlorosomes, which is attributed to the presence of a single 17^2-farnesyl-*R*-[E,M] BChl *d* homologue, as opposed to the mixture of BChl *c* homologues present in the WT. One of the objectives of this thesis has been to gather information about the structure of chlorosomes from the *bchQRU* mutant with MAS NMR as the primary tool, to gain insight into common denominators regarding structure and function of chlorosomes, and into differences between species (Chapter 4). The homogeneous composition of the mutants provides the added advantage of increased spectral resolution. In the *bchQRU* mutant there is no methyl group at position 20, unlike in BChl *c*, which enhances the ring planarity. This makes for a more tightly packed BChl arrangement in the chlorosomes produced by the genetically modified species.

Using 2D homonuclear and heteronuclear correlation experiments, it was possible to obtain the ^{1}H and ^{13}C chemical shift assignment of the self-assembled BChl *d* molecules in the *bchQRU* chlorosomes. Distance constraints that were resolved using the CHHC experiment revealed an alternating *syn-anti* stacking motif. The experimentally observed ^{1}H aggregation shifts were matched by calculated ring-current shifts. In general, proton shifts are more sensitive to the effects of aggregation, while carbon shifts are sensitive to the electronic structure. It was possible to rule out other structural models available in the literature, based on the

calculation of their proton ring-current shifts. New cryo-EM data that has become available reveals repeats in the *bchQRU* mutant of 0.83 nm, perpendicular to the direction of the 2.1 nm repeat that falls along the tube axis. The electron density projection image of a multi-tubular model constructed from several *syn-anti* stacks running perpendicular to the tube axis produces a simulated layer line pattern matching the experimental data, thereby validating our structural model.

It was possible to make an initial assessment of the structure of chlorosomes from the *bchQR* mutant of *C. tepidum* in direct comparison to the chlorosomes from the WT (Chapter 5). The *bchQR* mutant produces chlorosomes with a single 17^2-farnesyl-*R*-[E,M] BChl *c* homologue. The ^{13}C-^{13}C and ^{1}H-^{13}C NMR datasets are more complicated for this mutant. Two distinct sets of NMR peaks of approximately the same intensity are resolved for some positions in the BChl *c* ring. CHHC distance constraints resolved for this mutant favor *syn-anti* stacking, similar to the *bchQRU* mutant. Corresponding CHHC datasets for the WT do not have sufficient resolution, so it is difficult to determine whether the chlorosomes from the WT have the same microstructure as those of the mutants from NMR distance constraints. However, the combination of the shift analysis and the dimeric character that transpires from the EM contributes to converging evidence for the *syn-anti* building block as a possible common denominator in the stacking of the BChls in chlorosomes. The methyl group present at position 20 in BChl *c* causes additional ring deformation, the magnitude of which differs for *syn* and *anti* ligation. Chemical shift calculations of optimized *syn* and *anti* coordinated monomers partly explain the doubling of NMR signals observed. Additional data will allow validation of the structural models for the *bchQR* mutant and for the WT.

Another objective of this thesis has been to analyze the structure of two artificial pigment aggregates, *i.e.* zinc chlorins in the solid-state (Chapter 6), *sans* isotope enrichment. One of the two zinc chlorins has been shown to form chlorosome like tubular aggregates in solution [1]. Using natural abundance samples, it was possible to collect well resolved ^{1}H-^{13}C datasets, with which a ^{1}H chemical shift assignment and subsequent estimation of aggregation shifts for the chlorin rings was obtained. A good

match was found between experimental aggregation shifts and calculated ring-current shifts for the antiparallel monomer model. This shows that in the solid-state these chlorins aggregate in extended lamellae forming artificial antennae that are built of stacks in which the zinc chlorins are arranged in an antiparallel fashion. The stacks are held together either by H-bonds or a charge stabilization mechanism to form a 3D space filling structure.

7.2 Functional relevance

To explain the 0.83 and 1.25 nm layer lines observed with cryo-EM for the *bchQRU* mutant and the WT, with molecular modeling two configurations having stacks running perpendicular and parallel to the tube axis are deduced (Chapter 4). This creates a suprastructural framework that allows for the accommodation of chemical heterogeneity. The absorption spectra of the 17^2-farnesyl-*R*-[E,M] BChl *d* producing *bchQRU* mutant and the 17^2-farnesyl-*R*-[E,M] BChl *c* producing *bchQR* mutant are considerably narrower than for the WT [2]. This suggests that the varying methylation in the WT at 8^2 and 12^1 is important to increase the absorption cross-section. The broadening in the absorption spectrum of the WT in comparison to the mutants can be attributed to the different microenvironments of the homologues of BChl *c* that are present. The suprastructure with stacks running parallel to the tube axis must be sufficiently stable to accept BChl *c* with methyl or ethyl side chains at 12-C and ethyl, propyl, or isobutyl side chains at 8-C.

7.3 Future experiments

The elaborate route for synthesis of the chlorin compounds makes it expensive in terms of time and money to synthesize isotope enriched compounds in quantities sufficient for solid-state NMR analyses. As a result, when working from natural abundance samples the possibilities of nuclei that can directly be analyzed with solid-state NMR are limited to the protons which have a large natural abundance. In Chapter 6 it was

possible to obtain the proton shifts via the ^{1}H-^{13}C FSLG experiment. To obtain a dataset of sufficient resolution, the duration of the experiment tends to be rather long.

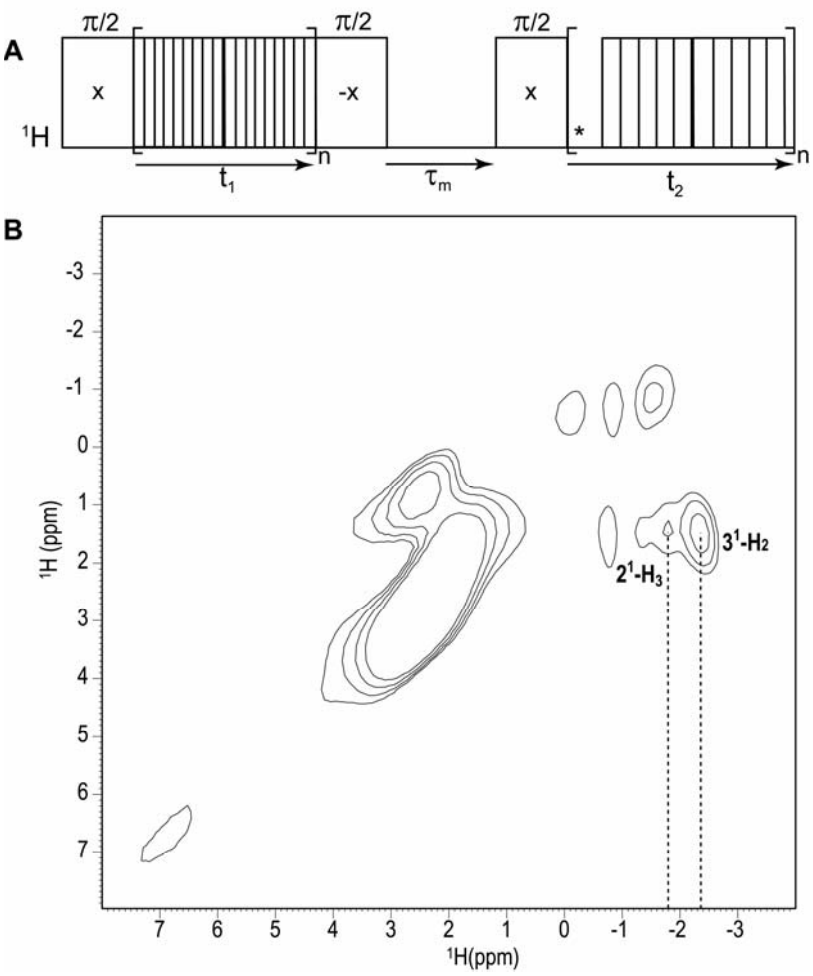

Figure 7.1 (A) Pulse sequence used for the 2D ^{1}H-^{1}H correlation experiment (Figure adapted from reference [3]). (B) 2D ^{1}H-^{1}H correlation spectra of natural abundance 3^{1} methoxy zinc chlorin, obtained using the pulse sequence represented in (A), with a mixing time of 100 μs. The experiment was performed at a spinning frequency of 14 kHz at a field of 17.6T.

Possible experiments that could be utilized in the future for a more rapid analysis of these unlabeled compounds are the 2D ^{1}H-^{1}H correlation experiments implemented with *ω*PMLG decoupling [3]. In this experiment as indicated in Figure 7.1A following a π/2 pulse the proton magnetization evolves during PMLG segment and is then transferred to the *z*-axis [4].

Magnetization exchange takes place during a mixing time τ_m, after which it is again transferred to the plane perpendicular to the effective chemical shift direction of the *w*PMLG detection period [3,4]. The *rf* amplitude is set to zero, indicated in the figure by an asterisk during two consecutive time segments enabling data acquisition. The initial experimental setup has been implemented and a first 2D test dataset has been acquired for a sample of natural abundance 3^1 methoxy zinc chlorin (Figure 7.1B, Chapter 6) at a mixing interval τ_m of 100 μs. Monitoring the intensities of the cross-peaks as a function of the mixing time in such 2D experiments can provide additional structural information for such unlabeled systems in a more rapid manner.

References

[1] V. Huber, M. Katterle, M. Lysetska and F. Würthner (**2005**) *Angewandte Chemie-International Edition* 44: 3147-3151.

[2] A. G. M. Chew, N. U. Frigaard and D. A. Bryant (**2007**) *Journal of Bacteriology* 189: 6176-6184.

[3] E. Vinogradov, P. K. Madhu and S. Vega (**2002**) *Chemical Physics Letters* 354: 193-202.

[4] E. Vinogradov, P. K. Madhu and S. Vega (**1999**) *Chemical Physics Letters* 314: 443-450.